

Relativistic coupled-cluster calculation of the electric dipole polarizability and correlation energy of Cn, Nh⁺, and Og: Correlation effects from lighter to superheavy elements

Ravi Kumar,¹ S. Chattopadhyay², D. Angom^{3,4} and B. K. Mani^{1,*}

¹*Department of Physics, Indian Institute of Technology, Hauz Khas, New Delhi 110016, India*

²*Department of Physics, Kansas State University, Manhattan, Kansas 66506, USA*

³*Department of Physics, Manipur University, Canchipur 795003, Manipur, India*

⁴*Physical Research Laboratory, Ahmedabad 380009, Gujarat, India*



(Received 4 March 2021; accepted 18 May 2021; published 1 June 2021)

We employ a relativistic coupled-cluster theory to compute the ground-state electric dipole polarizability α and the electron correlation energy of the superheavy elements Cn, Nh⁺, and Og. To assess the electron correlation trends with Z , we also compute the correlation energies of the three lighter homologs for each of the elements. In the computations, we use the Dirac-Coulomb-Breit Hamiltonian and incorporate the quantum electrodynamic corrections from the Uehling potential and the self-energy. The effects of triple excitations are considered perturbatively in the theory. Our recommended values of α are in good agreement with previous theoretical results. As expected, the dominant contribution is from the valence electrons. Except for Cn and Og, the contribution from the Breit interaction decreases with Z . For the vacuum polarization and self-energy corrections, the contributions increase with Z . To understand the correlation energy trends better, we also compute the correlation energy with the relativistic many-body perturbation theory.

DOI: [10.1103/PhysRevA.103.062803](https://doi.org/10.1103/PhysRevA.103.062803)

I. INTRODUCTION

The study of superheavy elements (SHEs) is a multidisciplinary research area which provides a roadmap to investigate and understand several properties related to physics and chemistry [1–6]. There is, however, a lack of experimental data on atomic properties of SHEs due to various challenges, such as low production rate, short half-lives of elements, and the lack of a state-of-the-art one-atom-at-a-time experimental facility associated with atomic experiments [1,7,8]. Moreover, the properties of SHEs cannot be predicted based on lighter homologs, as they often differ due to relativistic effects in SHEs [5]. In such cases, the theoretical investigations of physical and chemical properties provide important insight into the properties of SHEs. Moreover, the benchmark data on these properties from accurate theoretical predications is important for future experiments. Calculating accurate properties of SHEs is, however, a difficult task. The reason for this could be attributed to the competing nature of the relativistic and correlation effects in these systems. For a reliable prediction of the properties of SHEs, both of these effects should be incorporated at the highest level of accuracy. In addition, large basis sets should be used to obtain the converged properties' results.

The electric dipole polarizability, α , of an atom or ion is a key parameter used to probe several fundamental as well as technologically relevant properties in atoms and ions [9–14]. The α for SHEs Cn and Og has been calculated in previous works, Refs. [15–18] and [16,17,19,20], respectively. Though

most of these results are using the CCSD(T), there is a large variation in the reported values for both Cn and Og. For example, the value of α reported in CCSD(T) calculation [20] is $\approx 25\%$ larger than a similar calculation [19]. The reason for this can, perhaps, be attributed to the complex nature of the electron correlation and relativistic effects in these systems. The other point to be mentioned here is that the basis used in these calculations is not large. Moreover, the inclusion of the contributions from the Breit interaction and QED corrections is crucial to obtain accurate and reliable values of α for SHEs.

In this paper, we employ a fully relativistic coupled cluster (RCC) theory-based method to calculate the electric dipole polarizability and the electron correlation energy of SHEs Cn, Nh⁺, and Og. The superheavy element ${}_{118}^{294}\text{Og}$, synthesized in 2006 by heavy ion fusion reaction of ${}^{48}\text{Ca}$ with ${}^{249}\text{Cf}$ [21], is the heaviest element in the periodic table [22]. It has a half-life of $0.89_{-0.31}^{+1.07}$ ms [21], which poses challenges to the experimental studies of physical and chemical properties [7,8]. Cn, perhaps, is the most well-studied SHE. It was synthesized at Darmstadt in 1996 [23] where an isotope ${}_{112}^{277}\text{Cn}$, with a very short half-life of 240_{-90}^{+430} μs , was identified in the nuclear fusion reaction of ${}^{70}\text{Zn}$ with ${}^{208}\text{Pb}$. In subsequent experiments, Refs. [24–27], some other isotopes were discovered and their chemical properties were investigated. The experimental and theoretical studies predict the properties of Cn to be different from the lighter homologs [17,18,27]. The main reason for this is attributed to the large contraction of ns orbitals due to the poor screening of the nuclear charge. Nh is the first SHE in the p block of the periodic table. It was discovered at the RIKEN, Japan, in 2004 in the fusion reaction of ${}^{209}\text{Bi}$ with ${}^{70}\text{Zn}$ [28], where the produced isotope ${}_{113}^{287}\text{Nh}$ is reported to have a half-life of 0.34 ms. Like Cn, in terms of

*bkmani@physics.iitd.ac.in

TABLE I. The α_0 and β parameters of the even-tempered GTO basis used in our calculations.

Atom	s		p		d		f	
	α_0	β	α_0	β	α_0	β	α_0	β
Cn	0.00545	1.870	0.00475	1.952	0.00105	1.970	0.00380	1.965
Og	0.00410	1.910	0.00396	1.963	0.00305	1.925	0.00271	1.830
Nh ⁺	0.05200	1.912	0.03650	1.655	0.05550	1.945	0.00455	1.945

properties, it is predicted to show different trends than lighter homologs, due to the strong contraction and stabilization of $np_{1/2}$ orbitals. The large number of electrons in the SHEs poses serious theoretical challenges to account for the electron correlation effects accurately. This is on account of the exponential increase in electron configurations with the number of electrons. At the same time, the short lifetimes of the SHEs limits experimental possibilities and, hence, there is a need for reliable theoretical results. For this reason, to add to the theoretical understanding, we employ relativistic coupled-cluster (CC) theory to compute the structure and properties of these SHEs. In addition, this work establishes the applicability of our closed-shell relativistic CC method to capture the electron correlation effects in SHEs and, hence, gives reliable results for structure and properties.

RCC is one of the most powerful many-body theories for atomic structure calculations as it accounts for the electron correlation to all orders of residual Coulomb interaction. We have used this to calculate the many-electron wave function and the electron correlation energy. The effect of the external electric field, in the case of α , is accounted for using the perturbed relativistic coupled-cluster (PRCC) theory [29–33]. One of the key merits of PRCC in the properties calculation is that it does not employ the sum-over-state [34,35] approach to incorporate the effects of a perturbation. The summation over all the possible intermediate states is subsumed in the perturbed cluster operators. The leading order relativistic effects are accounted for using the four-component Dirac-Coulomb-Breit no-virtual-pair Hamiltonian [36]. And, the effects of Breit, QED, and triple excitations in CCs are computed using the implementations in our previous works [29,31–33]. Considering the importance of α , it has been computed using a variety of many-body methods in the literature. A recent

review article by Mitroy *et al.* [37] provides a summary of α for several atoms and ions computed using different methods. One reference, a tabulation of α for neutral atoms, which we have found very useful is Schwerdtfeger's updated table [38]. The table provides an exhaustive list of references on experimental and theoretical values of α for several neutral atoms.

To assess the trend of various electron correlation effects from lighter to SHEs, we also calculate the correlation energy and the contributions from the Breit and QED corrections to α for three lighter homologs in each SHE: Zn, Cd, and Hg in group 12; Ga⁺, In⁺, and Tl⁺ in group 13; and Kr, Xe, and Rn in group 18. Here, our main focus is to get deeper insight into various correlation effects as a function of Z in each of these SHEs. More precisely, we aimed to accurately calculate the value of α and correlation energy of SHEs Cn, Nh⁺, and Og using RCC and test the convergence of results with a very large basis; study the electron correlation in α for SHEs and assess the trend from lighter to SHEs; and examine in detail the contributions from the Breit and QED corrections to α for SHE elements and get a deeper insight to the trend of contributions from lighter homologs to SHEs.

The remaining part of the paper is organized into five sections. In Sec. II, we provide a brief description of the method used in the polarizability calculation. In Sec. III, we provide the calculational details such as the single-electron basis and computational challenges associated with polarizability calculation of SHEs. In Sec. IV, we analyze and discuss the results from our calculations. The theoretical uncertainty in our calculation is discussed in Sec. V. Unless stated otherwise, all the results and equations presented in this paper are in atomic units ($\hbar = m_e = e = 1/4\pi\epsilon_0 = 1$).

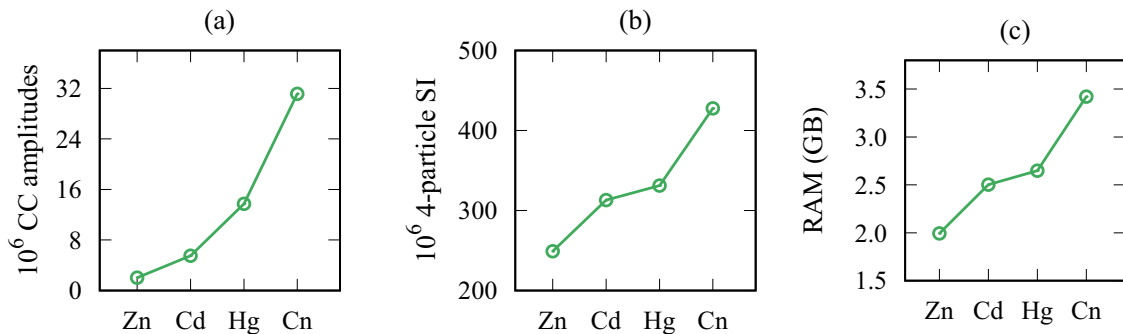


FIG. 1. (a) Number of cluster amplitudes, (b) number of four-particle Slater integrals, and (c) memory required to store four-particle Slater integrals, as a function of Z for group-12 elements.

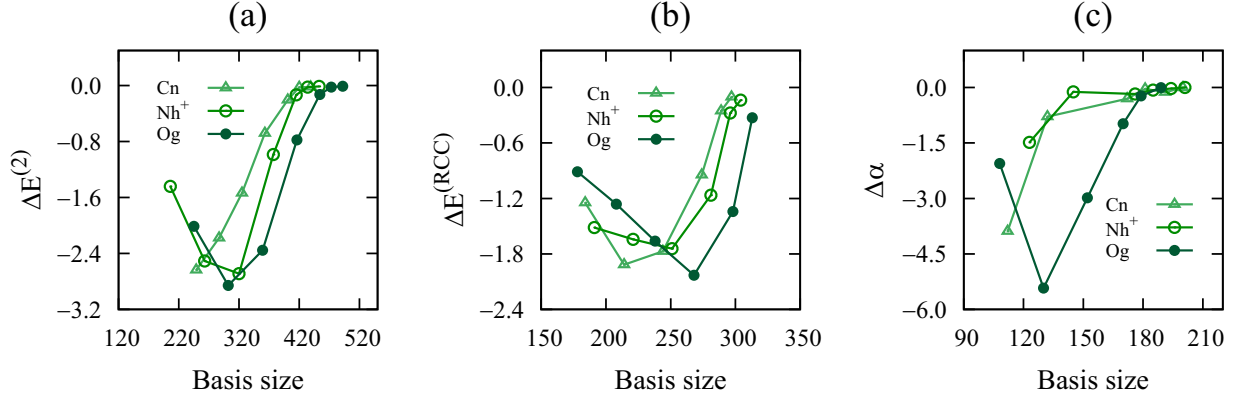


FIG. 2. Convergence of second-order correlation energy (a), the RCC energy (b), and α (c) as function of the basis size.

II. METHOD OF CALCULATION

The ground-state wave function of an N -electron atom or ion in RCC theory is

$$|\Psi_0\rangle = e^{T^{(0)}}|\Phi_0\rangle, \quad (1)$$

where $|\Phi_0\rangle$ is the Dirac-Fock (DF) reference wave function and $T^{(0)}$ is the closed-shell CC excitation operator. It is an eigenfunction of the Dirac-Coulomb-Breit no-virtual-pair Hamiltonian,

$$H^{\text{DCB}} = \sum_{i=1}^N [c\boldsymbol{\alpha}_i \cdot \mathbf{p}_i + (\beta_i - 1)c^2 - V_N(r_i)] + \sum_{i<j} \left[\frac{1}{r_{ij}} + g^{\text{B}}(r_{ij}) \right], \quad (2)$$

where $\boldsymbol{\alpha}$ and β are the Dirac matrices, and $V_N(r_i)$ is the nuclear potential. The negative-energy continuum states of the Hamiltonian are projected out by using the kinetically balanced finite Gaussian-type orbital (GTO) basis sets [39,40] and selecting only the positive energy states from the finite-size basis set [41,42]. The last two terms, $1/r_{ij}$ and $g^{\text{B}}(r_{ij})$, are the Coulomb and Breit interactions, respectively. For $g^{\text{B}}(r_{ij})$, we employ the expression [43]

$$g^{\text{B}}(r_{12}) = -\frac{1}{2r_{12}} \left[\boldsymbol{\alpha}_1 \cdot \boldsymbol{\alpha}_2 + \frac{(\boldsymbol{\alpha}_1 \cdot \mathbf{r}_{12})(\boldsymbol{\alpha}_2 \cdot \mathbf{r}_{12})}{r_{12}^2} \right]. \quad (3)$$

The operators $T^{(0)}$ in Eq. (1) are the solutions of the coupled nonlinear equations

$$\langle \Phi_a^p | H_N + [H_N, T^{(0)}] + \frac{1}{2!} [[H_N, T^{(0)}], T^{(0)}] + \frac{1}{3!} [[[[H_N, T^{(0)}], T^{(0)}], T^{(0)}], T^{(0)}] | \Phi_0 \rangle = 0, \quad (4a)$$

$$\langle \Phi_{ab}^{pq} | H_N + \frac{1}{2!} [[H_N, T^{(0)}], T^{(0)}] + \frac{1}{3!} [[[[H_N, T^{(0)}], T^{(0)}], T^{(0)}], T^{(0)}] + \frac{1}{4!} [[[[[H_N, T^{(0)}], T^{(0)}], T^{(0)}], T^{(0)}], T^{(0)}] | \Phi_0 \rangle = 0. \quad (4b)$$

Here, the states $|\Phi_a^p\rangle$ and $|\Phi_{ab}^{pq}\rangle$ are the singly and doubly excited determinants obtained by replacing *one* and *two* electrons from the core orbitals in $|\Phi_0\rangle$ with virtual orbitals, respectively. And $H_N = H^{\text{DCB}} - \langle \Phi_0 | H^{\text{DCB}} | \Phi_0 \rangle$ is the normal-ordered Hamiltonian.

In the presence of an external electric field, \mathbf{E}_{ext} , the ground-state wave function $|\Psi_0\rangle$ is modified due to interaction between induced electric dipole moment \mathbf{D} of the atom and \mathbf{E}_{ext} . We call the modified wave function the perturbed wave function, which in PRCC is defined as

$$|\tilde{\Psi}_0\rangle = e^{T^{(0)}} [1 + \lambda \mathbf{T}^{(1)} \cdot \mathbf{E}_{\text{ext}}] |\Phi_0\rangle, \quad (5)$$

where $\mathbf{T}^{(1)}$ is the perturbed CC operator and λ is a perturbation parameter. The wave function $|\tilde{\Psi}_0\rangle$ is an eigenstate of the modified Hamiltonian $H_{\text{Tot}} = H^{\text{DCB}} - \lambda \mathbf{D} \cdot \mathbf{E}_{\text{ext}}$. The perturbed CC operators $\mathbf{T}^{(1)}$ in Eq. (5) are the solutions of the linearized PRCC equations [29–32,44,45]:

$$\langle \Phi_a^p | H_N + [H_N, \mathbf{T}^{(1)}] | \Phi_0 \rangle = \langle \Phi_a^p | \mathbf{D} | \Phi_0 \rangle, \quad (6a)$$

$$\langle \Phi_{ab}^{pq} | H_N + [H_N, \mathbf{T}^{(1)}] | \Phi_0 \rangle = \langle \Phi_{ab}^{pq} | \mathbf{D} | \Phi_0 \rangle. \quad (6b)$$

The single and double excitations in the couple-cluster theory capture most of the correlation effects and, hence, the operators $T^{(0)}$ and $\mathbf{T}^{(1)}$ are approximated as $T^{(0)} = T_1^{(0)} + T_2^{(0)}$ and $\mathbf{T}^{(1)} = \mathbf{T}_1^{(1)} + \mathbf{T}_2^{(1)}$, respectively. This is referred to as the coupled-cluster single and double (CCSD) approximation [46]. In the present paper we, however, also incorporate the triple excitations perturbatively [29].

The perturbed wave function from Eq. (5) is used to calculate the ground-state polarizability. In PRCC,

$$\alpha = -\frac{\langle \tilde{\Psi}_0 | \mathbf{D} | \tilde{\Psi}_0 \rangle}{\langle \tilde{\Psi}_0 | \tilde{\Psi}_0 \rangle}. \quad (7)$$

Using the expression of $|\tilde{\Psi}_0\rangle$ from Eq. (5), we can write

$$\alpha = -\frac{\langle \Phi_0 | \mathbf{T}^{(1)\dagger} \bar{\mathbf{D}} + \bar{\mathbf{D}} \mathbf{T}^{(1)} | \Phi_0 \rangle}{\langle \Psi_0 | \Psi_0 \rangle}, \quad (8)$$

where $\bar{\mathbf{D}} = e^{T^{(0)\dagger}} \mathbf{D} e^{T^{(0)}}$ and, in the denominator, $\langle \Psi_0 | \Psi_0 \rangle$ is the normalization factor. Considering the computational

TABLE II. Electron correlation and total energies in atomic units for group-12, group-13, and group-18 elements. Listed RCC energies also include the contributions from the Breit and QED corrections.

	Basis		ΔE_{DC}		E_{total}	ΔE_{others}
	MBPT	RCC	MBPT	RCC		
Group 12						
Zn	336	206	-1.6769	-1.5690	-1796.1812	-1.6975 ^a , -1.6611 ^d -1.6206 ^f
Cd	461	223	-2.7278	-2.6216	-5595.9393	-2.7253 ^b , -2.6540 ^d -2.6500 ^f
Hg	413	227	-5.4681	-5.1164	-19653.9388	-5.4508 ^b , -5.2895 ^d -5.1760 ^f
Cn	439	289	-8.4393	-7.7981	-47335.9752	
Group 13						
Ga ⁺	411	227	-1.669	-1.58077	-1943.9435	
In ⁺	447	235	-2.744	-2.64147	-5882.8838	
Tl ⁺	409	220	-5.499	-5.15772	-20279.7851	
Nh ⁺	453	304	-8.4743	7.8439	-48517.6211	
Group 18						
Kr	413	255	-1.8532	-1.7900	-2790.3898	-1.8907 ^c , -1.8468 ^d -1.8466 ^e -1.8496 ^f
Xe	419	255	-3.0314	-2.9075	-7448.6635	-3.0877 ^c , -2.9587 ^d -2.9979 ^e -3.0002 ^f
Rn	372	245	-5.6195	-5.2945	-23601.3243	-5.7738 ^c , -5.5874 ^d -5.5250 ^f
Og	492	313	-8.9109	-8.3047	-54815.0764	

^aRef. [57] [MP2]; ^bRef. [58] [MP2]; ^cRef. [59] [MP2]; ^dRef. [60] [MP2]; ^eRef. [61] [RCC]; ^fRef. [62] [RCC].

complexity, we truncate $\bar{\mathbf{D}}$ and the normalization factor to second order in the cluster operators $T^{(0)}$. From our previous study [47], using an iteration scheme, we found that the terms with third and higher orders contribute much less to the properties.

III. CALCULATIONAL DETAIL

A. Single-electron basis

In the RCC and PRCC calculations, it is crucial to use an orbital basis set which provides a good description of the single-electron wave functions and energies. In the present paper, we use GTOs [39] as the basis. We optimize the orbitals as well as the self-consistent-field energies of GTOs to match the GRASP2K [48] results. In Table I, we provide the

values of the exponents α_0 and β [39] of the occupied orbital symmetries for Cn, Nh⁺, and Og. For further improvement, we incorporate the effects of Breit interaction, vacuum polarization, and self-energy corrections. This is crucial to obtain the value of the dipole polarizability of SHEs accurately, where the relativistic effects are larger due to higher Z . To compute the corrections from the vacuum polarization to the single-electron energies, we used Uehling potential [49], with the modification to incorporate the finite-size effect of nuclear charge distribution [50,51]:

$$V_{Ue}(r) = -\frac{2\alpha}{3r} \int_0^\infty dx x \rho(x) \int_1^\infty dt \sqrt{t^2 - 1} \left(\frac{1}{t^3} + \frac{1}{2t^5} \right) \times (e^{-2ct|(r-x)} - e^{-2ct(r+x)}). \quad (9)$$

Here, α is the fine structure constant and should not be confused with dipole polarizability, and $\rho(x)$ is the finite-size Fermi density distribution of the nuclear charge, expressed as

$$\rho_{nuc}(r) = \frac{\rho_0}{1 + e^{(r-c)/a}}, \quad (10)$$

with $a = t4 \ln(3)$. The parameter c is the half-charge radius such that $\rho_{nuc}(c) = \rho_0/2$, and t is the skin thickness. The corrections from the self-energy to single-electron energies are considered through the model Lamb-shift operator introduced by Shabaev *et al.* [52], using the code QEDMOD [53] developed by the same authors.

In the Appendixes, we compare the orbital energies of Cn (Table IX), Nh⁺ (Table X), and Og (Table XI) with GRASP2K [48] and B-spline [54] data. As seen from the tables, the GTO orbital energies are in excellent agreement with the numerical values from GRASP2K. The largest differences are 3.4×10^{-4} , 4.8×10^{-4} , and 9.2×10^{-4} Hartree in the case of $4f_{5/2}$, $1s_{1/2}$ and $2p_{1/2}$ orbitals of Cn, Nh⁺, and Og, respectively. The corrections from the vacuum polarization, $\Delta\epsilon_{Ue}$, and the self-energy, $\Delta\epsilon_{SE}$, to the orbital energies are provided in Table XII. Our results match well with the previous calculation [55] for Cn and Og.

B. Computational challenges with SHEs

The calculation of α for SHEs is a computationally challenging task. This is due to the large number of core electrons and the need for a larger basis size to obtain converged properties results. The latter pose three main hurdles in the calculations. First, the number of cluster amplitudes is very large, and solving the cluster equations requires long compute times. To give an example, as shown in Fig. 1, in the case of Cn, using a converge basis of 200 orbitals leads to more than 31 000 000 cluster amplitudes. This is about 2.3 times larger than the lighter atom Rn. Second, convergence of α with basis size is slow. This is in stark contrast to the convergence trends of α for lighter atoms and ions reported in our previous works [29,30,33]. For the lighter atoms and ions, convergence is achieved with a basis of 160 or less orbitals. However, for SHEs, convergence of α requires ≈ 200 orbitals. Third, storing the two-electron integrals for efficient computation requires large memory. Foratt instance, the number of *four-particle* two-electron integrals in the case of Cn is more than 427 000 000. This is about 1.3 times larger than the case of Rn. Moreover, in general parallelization,

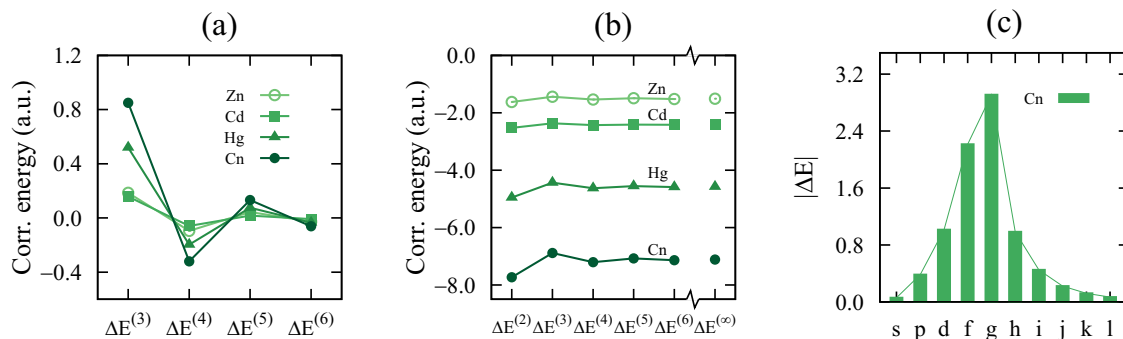


FIG. 3. (a) Third-, fourth-, fifth-, and sixth-order correlation energies, (b) cumulative correlation energy, and (c) contribution to correlation energy from orbitals of different symmetries. $\Delta E^{(\infty)}$ in (b) represents the infinite-order correlation energy and is equivalent to RCC energy.

solving the cluster equations requires storing the same set of integrals stored across all nodes. This leads to replication of data across compute nodes and puts severe restrictions on basis size in the PRCC calculations. To mitigate this problem, we have implemented a *memory-parallel-storage* algorithm [56] which avoids the storage replication of the integrals across different nodes. This allows efficient memory usage and uses a large orbital basis in the PRCC computations. The inclusion of perturbative triples to the computation of α enhances the computational complexity further. This is due to the evaluation of numerous additional polarizability diagrams arising from the perturbative triples. To illustrate the compute time, the computation of α for Cn using a basis of 200 orbitals without triples takes 120 h with 144 threads. Whereas, with partial triples included, it requires 280 h with 200 threads. Thus, the runtime more than doubled.

IV. RESULTS AND DISCUSSION

A. Convergence of α and correlation energy

The GTO basis, by definition, is mathematically incomplete [42]. Hence, it is essential to check the convergence of α and the correlation energy with basis size. Accordingly, the convergence trends of these quantities are shown in the Fig. 2. For efficiency, the computations are done with the Dirac-Coulomb Hamiltonian, as it is computationally less expensive than using the DCB Hamiltonian. To determine

the converged basis set, we start with a moderate basis size and add orbitals in each symmetry systematically. This is continued till the change in α and correlation energy is $\leq 10^{-3}$. For example, as discernible from Table VIII in the Appendixes, the change in α for Cn is 4.0×10^{-3} a.u. when the basis set is augmented from 191 to 200. So, to optimize the compute time, we consider the basis set with 191 orbitals as the optimal one for α . Once the optimal basis set is selected, in the further computations we incorporate the Breit interaction and QED corrections. As seen from Figs. 2(a) and 2(b), the convergence of the correlation energies requires a much larger basis. For example, for Cn, the converged second-order energy is obtained with the basis size of 439 (31s27p26d24f22g21h21i21j21k21l) orbitals. A similar trend is also observed for the other two SHEs and all the lighter homologs considered in this paper.

B. Correlation energy

The electron correlation energy in RCC is expressed as

$$\Delta E = \langle \Phi_0 | \bar{H}_N | \Phi_0 \rangle, \quad (11)$$

where $\bar{H}_N = e^{-T^{(0)}} H_N e^{T^{(0)}}$ is the similarity transformed Hamiltonian. In Table II, we list ΔE for SHEs and three lighter elements in each group. Since the correlation energies converge with very large basis sizes, it is not practical to use such large bases in the RCC calculations due to computational limitations. Some of the limitations are as mentioned

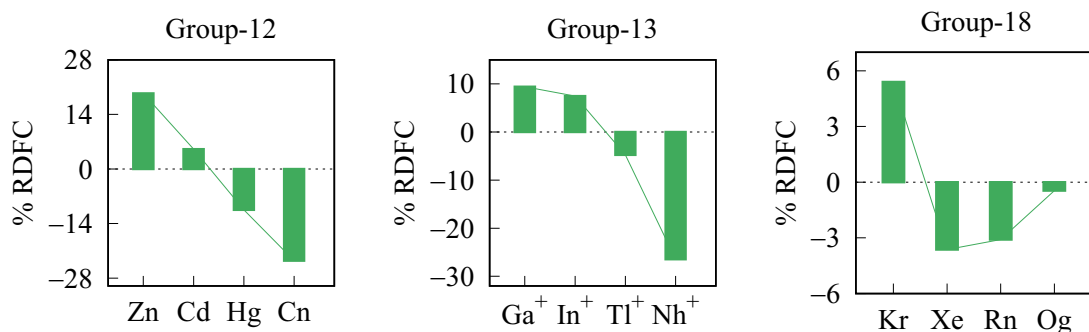


FIG. 4. In percentage, the *relative-DF-contribution* for group-12, group-13, and group-18 elements.

TABLE III. Final value of α (a.u.) from PRCC calculations compared with other theoretical data in the literature.

Element	Present paper		Other calculations	
	Method	α		
Cn	DF	35.234	25.82 ^a , 28.68 ^b ,	
	PRCC	26.944	27.40 ^d , 28 \pm 4 ^c	
	PRCC(T)	27.457		
	PRCC(T)+Breit	27.537		
	PRCC(T)+Breit+QED	27.588		
	Estimated	27.442		
	Recommended	27.44(88)		
Hg	PRCC(T)+Breit+QED	33.69(34)	31.32 ^g , 33.30 ^h , 33.44 ⁱ , 31.82 ^j , 34.42 ^k , 34.15 ^l , 33.6 ^m , 34.27 ⁿ , 33.75 ^o , 33.91(34) ^p 32.9 ^q , 39.1 ^c 34.73(52) ^r , 34.2(5) ^s 34.5(8) ^t	
	Nh ⁺	DF	23.182	
		PRCC	17.056	
		PRCC(T)	17.063	
		PRCC(T)+Breit	17.100	
		PRCC(T)+Breit+QED	17.135	
		Estimated	17.123	
	Recommended	17.12(55)		
	Tl ⁺	PRCC(T)+Breit+QED	20.13(12)	19.60 ^u 12.7(12) ^v
		Og	DF	56.197
PRCC	55.941		57.98 ^f , 57 \pm 3 ^c	
PRCC(T)	56.203			
PRCC(T)+Breit	56.250			
PRCC(T)+Breit+QED	56.545			
Estimated	56.536			
Recommended	56.54(181)			
Rn	PRCC(T)+Breit+QED	35.53(36)	33.18 ^w , 34.43 ^x 28.6 ^b , 32.6 ^y 34.2 ^c , 35.47 ^z 35.87 ^a , 34.89 ^{β} 34.60 ^{γ} , 35.04(1.80) ^{ϵ}	

^aRef. [15] [CCSD(T)]; ^bRef. [16] [CCSD(T)]; ^cRef. [17] [RRPA];
^dRef. [18] [DC-CCSD(T)]; ^eRef. [19] [R, DC-CCSD(T)]; ^fRef. [20] [R, Dirac+Gaunt, CCSD(T)]; ^gRef. [63] [CICP]; ^hRef. [64] [CASPT2]; ⁱRef. [65] [QCISD(T)]; ^jRef. [66] [CCSD(T)]; ^kRef. [15] [CCSD(T)]; ^lRef. [18] [CCSD(T)]; ^mRef. [67] [CCSD(T)]; ⁿRef. [68] [CCSDT + QED]; ^oRef. [69] [Expt.]; ^pRef. [70] [Expt.]; ^qRef. [71] [semi-emp.]; ^rRef. [72] [CCSD(T)]; ^sRef. [73] [CCSD(T) + Breit]; ^tRef. [74] [CCSD(T)]; ^uRef. [75] [CI+All-order]; ^vRef. [76] [Sum-rule]; ^wRef. [77] [MBPT]; ^xRef. [78] [CCSDT]; ^yRef. [79] [DK, CASPT2]; ^zRef. [80] [CCSD, ECP]; ^aRef. [81] [R, DFT, DC, PBE38]; ^{β} Ref. [82] [R, DKH2, B3LYP, SAR]; ^{γ} Ref. [83] [SOPP, CCSD(T) + MP2]; ^{ϵ} Ref. [19] [CCSD(T)].

in the previous section. To mitigate this, and to account for correlation energy from the virtual orbitals excluded in the RCC calculations, we resort to the second-order MBPT method. The RCC results of the ΔE listed in Table II are calculated using the expression

$$\Delta E_{\text{RCC}} \approx \Delta E_{\text{RCC}}^{\text{nconv}} + (\Delta E_{\text{MBPT}}^{\text{conv},2} - \Delta E_{\text{MBPT}}^{\text{nconv},2}), \quad (12)$$

TABLE IV. Contributions to α (in a.u.) from different terms in PRCC theory.

Terms + H.c.	Cn	Nh ⁺	Og
$\mathbf{T}_1^{(1)\dagger} \mathbf{D}$	34.5267	21.3767	68.9516
$\mathbf{T}_1^{(1)\dagger} \mathbf{D} \mathbf{T}_2^{(0)}$	-3.0095	-1.7444	-4.0179
$\mathbf{T}_2^{(1)\dagger} \mathbf{D} \mathbf{T}_2^{(0)}$	1.7485	0.7622	3.1900
$\mathbf{T}_1^{(1)\dagger} \mathbf{D} \mathbf{T}_1^{(0)}$	-0.0389	-0.0809	-1.5258
$\mathbf{T}_2^{(1)\dagger} \mathbf{D} \mathbf{T}_1^{(0)}$	-0.1087	-0.0247	0.2319
Normalization	1.2292	1.1898	1.1946
Total	26.9435	17.0524	55.9432

where $\Delta E_{\text{RCC}}^{\text{nconv}}$ is the correlation energy computed using RCC with orbitals up to j symmetry, and $\Delta E_{\text{MBPT}}^{\text{nconv},2}$ and $\Delta E_{\text{MBPT}}^{\text{conv},2}$ are the second-order energies calculated using RCC basis and a converged basis which includes orbitals up to l symmetry, respectively.

For all the elements listed in Table II, we observe an important trend in the correlation energy. The RCC correlation energy is smaller in magnitude than the second-order correlation energy. A similar trend was also observed in a previous work [62]. Based on our computations, this is due to the cancellations from higher order corrections subsumed in RCC. This is discernible for the group-12 elements in Fig. 3(a), where we have plotted the higher order contributions. These oscillate in sign and, hence, cancellations occur. As a result, the correlation energy oscillates initially before converging to the RCC value. This trend is visible in the plots of the cumulative contributions shown in Fig. 3(b). For the lighter elements, our RCC correlation energies are in good agreement with the previous RCC results [61,62]. The small difference could be attributed to the contributions from the Breit interaction and QED corrections included in the present work. For second-order correlation energies, there are four results from previous studies [57–60]. Our results match very well for all the elements.

Examining the symmetrywise contributions from virtual orbitals, we find that all three SHEs exhibit similar trends. This is not surprising as all are closed-shell systems. As discernible from the histograms in Fig. 3, contribution to the correlation energy increases initially as a function of orbital symmetry and then decreases. The first two dominant contributions, $\approx 35\%$ and 26% of the total correlation energy, arise from the g and f orbitals. The next two are from the d and h symmetries—their contributions are $\approx 12\%$ each for all the SHEs. The contribution from the virtuals with l symmetry is about 0.8% . This non-negligible contribution from the l symmetry orbitals indicates that the inclusion of the orbitals from higher symmetries is essential to obtain accurate energies for SHEs.

C. Polarizability

The values of α for SHEs with different methods subsumed in the PRCC theory are listed in Table III. The DF contribution is computed using Eq. (8) with $\mathbf{T}^{(1)}$ and $\bar{\mathbf{D}}$ replaced by the bare dipole operator \mathbf{D} , and is expected to have the dominant contribution. The PRCC values are the converged

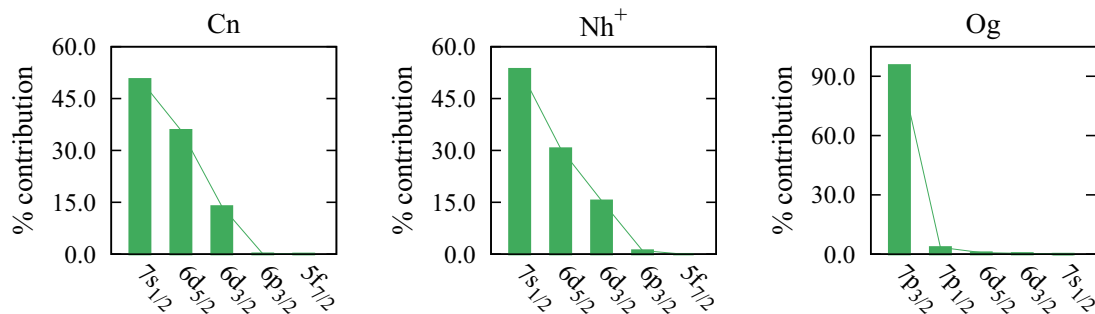


FIG. 5. Five largest percentage contributions from core orbitals to LO term $\{\mathbf{T}_1^{(1)\dagger} \mathbf{D} + \text{H.c.}\}$.

values from Table VIII, calculated using the DC Hamiltonian with a basis up to h symmetry. The values listed as *estimated* include the estimated contribution from the orbitals of i , j , and k symmetries. For this, we use a basis set of moderate size from Table VIII and then augment it with orbitals from i , j , and k symmetries to calculate percentage contribution; this is added to the PRCC value. To the best of our knowledge, there are no experimental data on α for SHEs considered in the present paper. However, to understand the trend of electron correlation effects, we compare our results with previous theoretical results. One important and crucial difference between previous studies and the present paper is the absence of QED corrections in previous works. Though the Breit interaction is included in previous work [15] for Cn, the contribution is not given explicitly. These corrections are, however, important to obtain the accurate and reliable values of α for SHEs. From our calculations, we find that the combined Breit + QED contributions are $\approx 0.5\%$, 0.4% , and 0.6% , respectively, for Cn, Nh⁺, and Og. Considering the important prospects associated with accurate data on α for SHEs, these are significant contributions and cannot be neglected.

For Cn, three of the previous studies, similar to the present paper, use CCSD(T). There are, however, important differences in terms of the basis used in these calculations. This could account for the difference in the values of α reported in these works. In Ref. [15], a relativistic basis with $11s8p8d4f$ orbitals optimized using pseudopotential Hartree-Fock energy is used and reports the smallest value 25.82. The other CCSD(T) result 27.40 from Ref. [18] uses a relatively larger

basis of $26s24p18d13f5g2h$. In terms of methodology and basis, Ref. [18] is the closest to the present work. Our recommended value 27.44(88) is close to this. The other CCSD(T) result of 28.68 is from the Ref. [16], which is obtained using an uncontracted Cartesian basis. This is the highest theoretical value reported in the literature. The other value 28 ± 4 is obtained using the RRPA [17] and this is close to our result. This is to be expected as both RRPA and PRCC account for core polarization, which is the dominant contribution to α after the DF. For the triple contribution to α , there is no clear trend in the previous RCC results. In Refs. [15,18], the contribution from triples reported as -0.08 and -0.07% of the CCSD value, respectively, and decrease the value of α . However, a positive contribution of $\approx 0.25\%$ is reported in Ref. [16]. In the present paper, we obtain a positive contribution of $\approx 1.9\%$, which increases the value of α further.

For Nh⁺, there are no previous theoretical results. The present paper reports the theoretical result of α , using PRCC theory. As we observed from Table III, though it has the same electronic structure as Cn, the value of α is smaller. This is attributed to the relativistic contraction of the $7s_{1/2}$ orbital due to increased nuclear potential. Like the case of Cn, the inclusion of partial triples increases the value of α further.

For Og, there are three previous results based on calculations using CCSD(T). Though the same methods are used, there is a large difference in the values of α reported in these works. For instance, the CCSD(T) value 57.98 reported in Ref. [20] is $\approx 25\%$ larger than the result in Ref. [19]. The reason for this could be attributed to the different types of

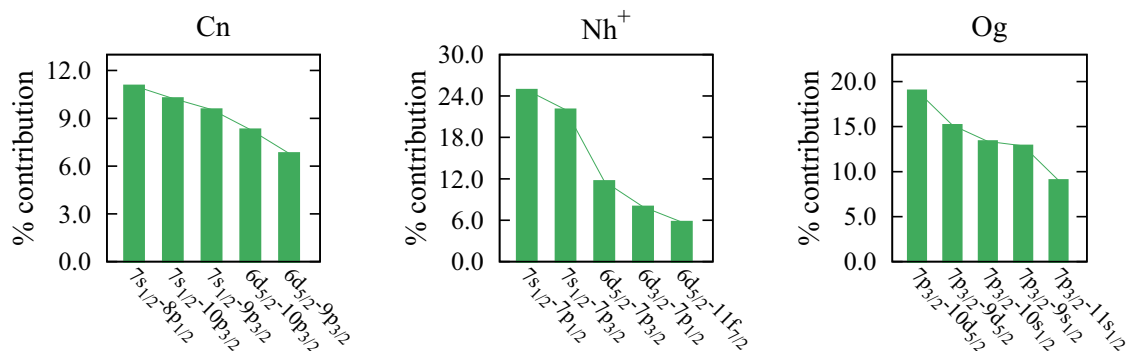


FIG. 6. In percentage, five dominant dipolar mixing of cores with virtuals.

TABLE V. Five leading contributions to NLO term $\{\mathbf{T}_1^{(1)\dagger} \mathbf{D} \mathbf{T}_2^{(0)} + \text{H.c.}\}$ (in a.u.) for α from core-core orbital pairs. This includes the pair-correlation contributions.

Cn	Nh ⁺
-0.618(7s _{1/2} , 6d _{5/2})	-0.420(7s _{1/2} , 6d _{5/2})
-0.479(7s _{1/2} , 7s _{1/2})	-0.243(7s _{1/2} , 7s _{1/2})
-0.405(6d _{5/2} , 6d _{5/2})	-0.235(7s _{1/2} , 6d _{3/2})
-0.337(6d _{5/2} , 7s _{1/2})	-0.204(6d _{5/2} , 6d _{5/2})
-0.327(7s _{1/2} , 6d _{3/2})	-0.171(6d _{5/2} , 7s _{1/2})
Og	
-2.805(7p _{3/2} , 7p _{3/2})	
-0.446(7p _{3/2} , 7p _{1/2})	
-0.365(7p _{3/2} , 6d _{5/2})	
-0.167(7p _{3/2} , 6d _{3/2})	
-0.114(7p _{1/2} , 7p _{3/2})	

bases used. In Ref. [19], the computations used the Faegri basis with 26s24p18d13f5g2h orbitals, however, in Ref. [20], an uncontracted relativistic quadrupole-zeta basis is used. The other CCSD(T) result 52.43 from Ref. [16] lies between the other two results. Our recommended value 56.54(181) is closer to the RRPA value 57(3) from Ref. [17] and CCSD(T) value, 57.98, from Ref. [20]. As mentioned in the case of Cn, this is due to the core-polarization effect accounting for all orders in both CCSD and RRPA. The obtained contribution from partial triples 0.47% is consistent with the contribution 0.66% reported in Ref. [19].

The value of α for lighter homologs for each of these SHEs using PRCC are reported in our previous works, Ref. [31] for group-12, Ref. [29] for group-13, and Ref. [30] for group-18 elements. In these references, we have presented comprehensive analyses on α in terms of electron correlations and detailed comparisons with previous theoretical and experimental results. We have also provided the details of the associated theoretical uncertainties. In the present paper, to illustrate the numerical quality of the computed α for SHEs, we list α for the adjacent lighter homolog for each of the SHEs–Hg for Cn, Tl⁺ for Nh⁺, and Rn for Og—in Table III. Among the three, Hg is both theoretically and experimentally well studied. For Nh⁺ and Rn, to the best of our knowledge, there are no experimental data for comparison. As evident from the table, our PRCC(T) + Breit + QED results

TABLE VI. Five leading contributions to $\{\mathbf{T}_1^{(1)\dagger} \mathbf{D} + \text{H.c.}\}$ (in a.u.) for α from core orbitals. This includes the DF and core-polarization contributions.

Cn	Nh ⁺	Og
17.468(7s _{1/2})	11.440(7s _{1/2})	65.874(7p _{3/2})
12.374(6d _{5/2})	6.534(6d _{5/2})	2.392(7p _{1/2})
4.776(6d _{3/2})	3.308(6d _{3/2})	0.562(6d _{5/2})
0.052(6p _{3/2})	0.224(6p _{3/2})	0.264(6d _{3/2})
0.015(5f _{7/2})	0.002(5f _{7/2})	0.042(7s _{1/2})

are in good agreement with the previous results for all three elements.

V. ELECTRON CORRELATION, BREIT, AND QED CORRECTIONS

In this section, we analyze and present the trends of electron correlation effects from the residual Coulomb interaction, Breit interaction, and QED corrections to α as function of Z .

A. Residual Coulomb interaction

To assess the correlation effects from residual Coulomb interaction, we define *relative-DF-contribution* (RDFC) as

$$\text{RDFC} = \frac{\alpha_{\text{PRCC}} - \alpha_{\text{DF}}}{\alpha_{\text{DF}}},$$

plotted in Fig. 4. As seen in the figure, the group-12 and group-13 elements show similar trends. For these groups, the RDFC is positive initially and then changes to negative. This is due to the changes in the core polarization effects as a function of Z , and can be attributed to the differences in the screening of nuclear potential. In each group, the core polarization contribution is positive for the first two elements and negative for the last two. The negative contribution makes the PRCC value of α lower than the DF value. A similar trend is also reported in previous works [15,16,18], where the DF value for Cn is higher than the CCSD value. For the group-18 elements, the RDFC shows a different trend. Except for Kr, it is negative for all other elements. In addition, the magnitude decreases from Xe to Og. This could be attributed to the negative and decreasing core polarization contributions

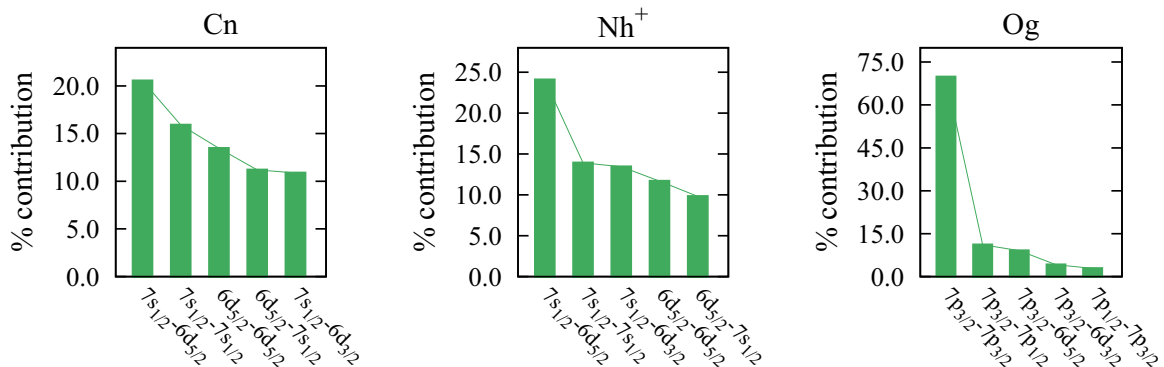


FIG. 7. Five largest percentage contributions from core-core orbital pairs to NLO term.

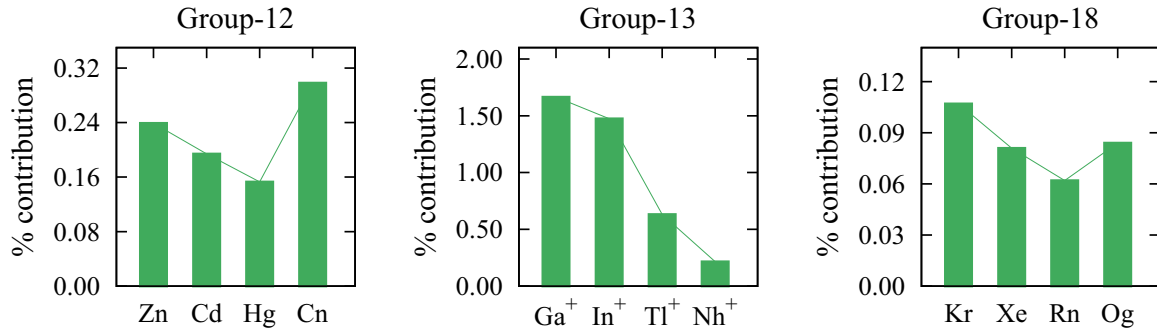


FIG. 8. Percentage contribution from Breit interaction to group-12, group-13, and group-18 elements.

from Xe to Og. Our DF result, 56.20, for Og is consistent with the previous results in Refs. [16,19]. These works reported DF values of 54.46 and 50.01, respectively, larger than the CCSD values. The difference in the DF values could be due to the different bases used in these calculations, and this can also be cause for the difference in the α values with the correlation effects.

To gain further insights into the electron correlations effects subsumed in the PRCC theory, we examine the contributions from different terms. These are listed in the Table IV. As seen from the table, for all SHEs, the LO contribution is from the term $\{\mathbf{T}_1^{(1)\dagger}\mathbf{D} + \text{H.c.}\}$. This is to be expected, as it subsumes the contributions from DF and RPA. The contributions are larger than PRCC by $\approx 28\%$, 25% , and 23% for Cn, Nh^+ , and Og, respectively. The contribution from the NLO term $\{\mathbf{T}_1^{(1)\dagger}\mathbf{D}\mathbf{T}_2^{(0)}\}$ is small and opposite in phase to the LO term. It accounts for $\approx -11\%$, -10% , and -7% of the PRCC values for Cn, Nh^+ , and Og, respectively. The next to NLO (NNLO) term is $\mathbf{T}_2^{(1)\dagger}\mathbf{D}\mathbf{T}_2^{(0)}$ and contributes $\approx 6\%$, 4% , and 6% of the PRCC value. The contributions from the other terms are small, and the reason is the smaller magnitude of the $\mathbf{T}_1^{(0)}$ CC operators.

To examine in more detail, we assess the contributions from the core-polarization and pair-correlation effects, con-

TABLE VII. Contributions to α from Breit interaction, vacuum polarization, and the self-energy corrections in atomic units.

Elements	Z	Breit interactions	Self-energy	Vacuum polarization
Group 12				
Zn	30	-0.0928	0.0221	-0.0038
Cd	48	-0.0953	0.0648	-0.0159
Hg	80	0.0519	0.0933	-0.0358
Cn	112	0.0802	0.1072	-0.0557
Group 13				
Ga^+	31	-0.3006	0.0090	-0.0018
In^+	49	-0.3647	0.0249	-0.0070
Tl^+	81	-0.1283	0.0526	-0.0274
Nh^+	113	0.0366	0.0794	-0.0440
Group 18				
Kr	36	0.0179	0.0011	0.0009
Xe	54	0.0213	0.0042	0.0031
Rn	86	0.0226	0.0239	0.0181
Og	118	0.0472	0.1162	0.1769

tributions are shown in the Tables V and VI, respectively. For the core polarization, we identify five dominant contributions to the LO term and these are listed in Table VI. Since Cn and Nh^+ have the same ground-state electronic configuration, both show similar correlation trends. For both, the most dominant contribution is from the valence orbital $7s_{1/2}$ and this is due to its larger radial extent. As shown in Fig. 5, the contribution from $7s_{1/2}$ is $\approx 50\%$ and 53% of the LO value for Cn and Nh^+ , respectively. For Cn, we find that more than 60% of the $7s_{1/2}$ contributions arise from $\mathbf{T}_1^{(1)}$ involving the $8p_{1/2}$, $10p_{3/2}$, and $9p_{3/2}$ orbitals. Whereas for Nh^+ , the $7p_{1/2}$ and $7p_{3/2}$ together contribute more than 87% of the total contribution. The next

TABLE VIII. Convergence trend of α calculated using the Dirac-Coulomb Hamiltonian as a function of basis size.

Basis	Orbitals	α
Cn		
90	14s, 11p, 10d, 8f, 6g, 3h	32.772
112	16s, 13p, 12d, 10f, 8g, 5h	28.884
132	18s, 15p, 14d, 12f, 9g, 7h	28.094
152	20s, 17p, 16d, 14f, 11g, 8h	27.418
172	22s, 19p, 18d, 16f, 13g, 9h	27.116
181	23s, 20p, 19d, 17f, 14g, 9h	27.078
191	25s, 21p, 20d, 18f, 15g, 9h	26.948
200	26s, 22p, 21d, 19f, 16g, 9h	26.944
Nh^+		
101	15s, 13p, 12d, 8f, 5g, 5h	19.493
123	17s, 15p, 14d, 10f, 7g, 7h	18.009
145	19s, 17p, 16d, 12f, 9g, 9h	17.889
167	21s, 19p, 18d, 14f, 11g, 11h	17.330
176	22s, 20p, 19d, 15f, 12g, 11h	17.155
185	23s, 21p, 20d, 16f, 13g, 11h	17.082
194	24s, 22p, 21d, 17f, 14g, 11h	17.053
201	25s, 23p, 22d, 18f, 14g, 11h	17.053
Og		
86	14s, 12p, 9d, 7f, 5g, 3h	67.613
108	16s, 14p, 11d, 9f, 7g, 5h	65.556
130	18s, 16p, 13d, 11f, 9g, 7h	60.134
152	20s, 18p, 15d, 13f, 11g, 9h	57.149
170	22s, 20p, 17d, 15f, 12g, 10h	56.170
179	23s, 21p, 18d, 16f, 13g, 10h	55.943
189	25s, 22p, 19d, 17f, 14g, 10h	55.941

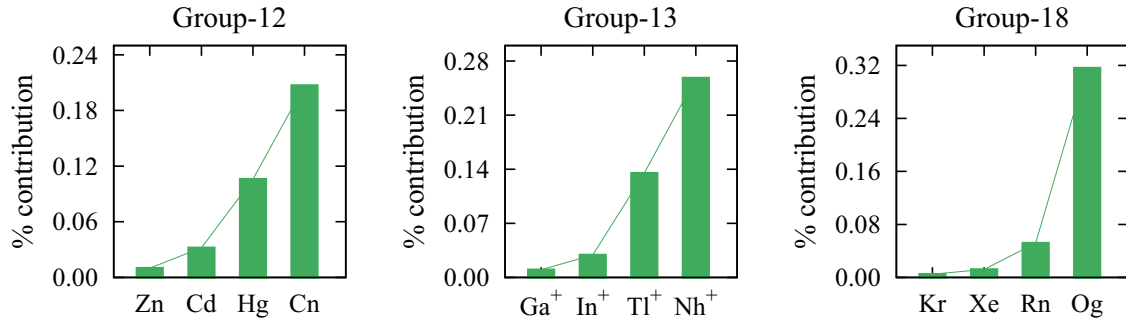


FIG. 9. Percentage contribution from vacuum polarization to group-12, group-13, and group-18 elements.

two important contributions are from the core orbitals $6d_{5/2}$ and $6d_{3/2}$. The contribution from the former is almost double the latter. In particular, for Cn and Nh^+ , the contributions from $6d_{5/2}$ is 35% and 30%, respectively, whereas, the contribution from $6d_{3/2}$ is $\approx 14\%$ and 15% , respectively. The larger contribution from $6d_{5/2}$ could be attributed to the strong dipolar mixing with $10p_{3/2}$ and $9p_{3/2}$ for Cn, and $7p_{3/2}$ and $11f_{7/2}$ for Nh^+ (see Fig. 6).

For Og, compared to Cn and Nh^+ , we observe a different trend of core-polarization effect. More than 95% of the contribution from the LO term arises from valence orbital $7p_{3/2}$. The other valence and core orbitals contribute less than 5% and $7p_{1/2}$ contributes only $\approx 3\%$ of the LO term. The reason for this could be the larger radial extent of the $7p_{3/2}$ orbital as $7p_{1/2}$ orbital contracts due to relativistic effects. The five dominant contributions arise from the dipolar mixing of $7p_{3/2}$ with $10d_{5/2}$, $9d_{5/2}$, $10s_{1/2}$, $9s_{1/2}$, and $11s_{1/2}$ orbitals. These orbitals together contribute $\approx 73\%$ of the total contribution (see Fig. 6).

To assess the contribution from pair-correlation effects, we consider the NLO term and identify the dominant contributions to it. These are listed in Table V in terms of the pairs of core orbitals and these correspond to the $T_2^{(0)}$ with dominant contributions. This is an appropriate approach as the most dominant term involving doubly excited cluster operators is the NLO term. For better illustration, the percentage contributions to those listed in Table V are plotted in the Fig. 7. For both Cn and Nh^+ , the first two dominant contributions are from the $(7s_{1/2}, 6d_{5/2})$ and $(7s_{1/2}, 7s_{1/2})$ core-orbital pairs. In percentage, these are $\approx -20\%$ and -16% for Cn, whereas $\approx -24\%$ and -14% for Nh^+ . Though the next three contri-

butions are from the same core-orbital pairs, $(6d_{5/2}, 6d_{5/2})$, $(6d_{5/2}, 7s_{1/2})$, and $(7s_{1/2}, 6d_{3/2})$, in both elements there are differences in terms of the order in which they contribute. Like in the core-polarization effect, we observe a different trend for Og. About 70% of the total contribution is from only the $(7p_{3/2}, 7p_{3/2})$ orbital pair.

B. Breit and QED corrections

To analyze the trend of correlation effects arising from the Breit interaction, vacuum polarization and the self-energy corrections as a function of Z , we separate the contributions from these interactions. These are listed in Table VII. In addition, for comparison and to show the trends in the group, the percentage contributions from the corresponding groups in the periodic table of the SHEs are shown in Figs. 8–10, respectively. For the Breit interaction, as we see from Fig. 8, except for Cn and Og, we observe a trend of decreasing contributions with increasing Z within the groups. One feature common to all SHEs is that the contributions have the same phase as PRCC and hence increase the value of α . For lighter elements, however, there is no clear trend.

For the corrections from the vacuum polarization and self-energy, from Figs. 9 and 10 we see that the contribution from both the vacuum polarization and self-energy increases with Z for all three groups. This is as expected. For the vacuum polarization, the effect is larger due to higher nuclear charge Z . For the self-energy, the correction depends on the energy of the orbital, which again depends on the nuclear charge. In terms of the phase of the contributions from vacuum polarization, these are opposite to PRCC value for all the elements

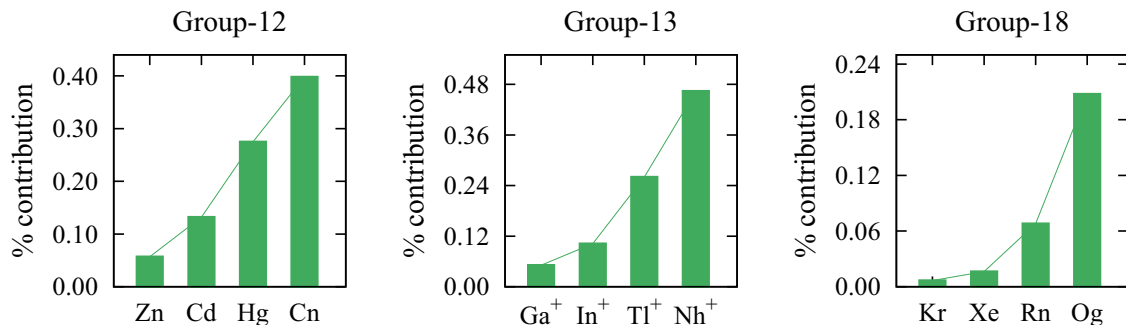


FIG. 10. Percentage contributions from self-energy correction to group-12, group-13, and group-18 elements.

TABLE IX. Orbital energies for core orbitals (in Hartree) from GTO is compared with the GRASP2K and B-spline energies for Cn. Here [x] represents multiplication by 10^x .

Orbital	GRASP2K	B spline	GTO
$1s_{1/2}$	7070.83320	7071.11186	7070.83326
$2s_{1/2}$	1444.87110	1444.92899	1444.87138
$3s_{1/2}$	390.81374	390.82783	390.81406
$4s_{1/2}$	113.44660	113.45069	113.44692
$5s_{1/2}$	30.05645	30.05764	30.05670
$6s_{1/2}$	5.68070	5.68099	5.68070
$7s_{1/2}$	0.45115	0.45119	0.45114
$2p_{1/2}$	1405.71950	1405.72953	1405.71920
$3p_{1/2}$	371.98098	371.98361	371.98109
$4p_{1/2}$	104.23703	104.23780	104.23723
$5p_{1/2}$	25.88719	25.88738	25.88726
$6p_{1/2}$	4.12316	4.12320	4.12312
$2p_{3/2}$	1007.09780	1007.09651	1007.09804
$3p_{3/2}$	274.99360	274.99302	274.99388
$4p_{3/2}$	76.37753	76.37735	76.37776
$5p_{3/2}$	17.99726	17.99719	17.99718
$6p_{3/2}$	2.41564	2.41562	2.41564
$3d_{3/2}$	245.88774	245.88719	245.88802
$4d_{3/2}$	62.08615	62.08599	62.08641
$5d_{3/2}$	11.85266	11.85260	11.85259
$6d_{3/2}$	0.56273	0.56271	0.56273
$3d_{5/2}$	229.40040	229.39991	229.40069
$4d_{5/2}$	57.56171	57.56155	57.56196
$5d_{5/2}$	10.70702	10.70697	10.70692
$6d_{5/2}$	0.44208	0.44207	0.44208
$4f_{5/2}$	38.82989	38.82975	38.83023
$5f_{5/2}$	3.33495	3.33492	3.33493
$4f_{7/2}$	37.51594	37.51581	37.51628
$5f_{7/2}$	3.09251	3.09247	3.09248

TABLE X. Orbital energies for core orbitals (in Hartree) from GTO is compared with the GRASP2K and B-spline energies for Nh^+ . Here [x] represents multiplication by 10^x .

Orbital	GRASP2K	B spline	GTO
$1s_{1/2}$	7245.8727391	7246.182976	7245.873218
$2s_{1/2}$	1487.4479289	1487.512728	1487.448327
$3s_{1/2}$	403.5128636	403.529178	403.513164
$4s_{1/2}$	117.9615376	117.966271	117.961704
$5s_{1/2}$	31.8304473	31.831827	31.830498
$6s_{1/2}$	6.4543326	6.454659	6.454278
$7s_{1/2}$	0.8293919	0.829453	0.829389
$2p_{1/2}$	1448.2662707	1448.277353	1448.266677
$3p_{1/2}$	384.4936370	384.497093	384.493911
$4p_{1/2}$	108.6076330	108.608617	108.607744
$5p_{1/2}$	27.5681904	27.568442	27.568231
$6p_{1/2}$	4.8384890	4.838538	4.838465
$2p_{3/2}$	1028.6629340	1028.661537	1028.663316
$3p_{3/2}$	282.2280516	282.227605	282.228310
$4p_{3/2}$	79.1393402	79.139197	79.139459
$5p_{3/2}$	19.1605082	19.160449	19.160489
$6p_{3/2}$	2.9774011	2.977385	2.977406
$3d_{3/2}$	252.7000748	252.699678	252.700378
$4d_{3/2}$	64.6075721	64.607451	64.607745
$5d_{3/2}$	12.8763169	12.876269	12.876364
$6d_{3/2}$	1.0204591	1.020450	1.020479
$3d_{5/2}$	235.5220171	235.521671	235.522311
$4d_{5/2}$	59.8711971	59.871089	59.871368
$5d_{5/2}$	11.6644138	11.664335	11.664411
$6d_{5/2}$	0.8811957	0.881171	0.881195
$4f_{5/2}$	40.8372335	40.837027	40.837249
$5f_{5/2}$	4.0945793	4.094568	4.094589
$4f_{7/2}$	39.4570885	39.456886	39.457103
$5f_{7/2}$	3.8335434	3.833539	3.833556

of group 12 and group 13, and hence lowers the value of α . For group 18, however, we observe the contributions of the same phase as PRCC. In terms of magnitude, the contributions are $\approx 0.21\%$, 0.26% , and 0.31% of the PRCC value for Cn, Nh^+ , and Og, respectively. For the self-energy, one prominent feature of the contributions we observe is that it is positive for all elements in all three groups and therefore increases the value of α . The contributions in the case of Cn, Nh^+ , and Og are $\approx 0.4\%$, 0.5% , and 0.2% of the PRCC values, respectively.

C. Theoretical uncertainty

In this section, we discuss the theoretical uncertainty associated with our results for α . For this, we have identified four sources. The first source of uncertainty is the truncation of the basis set used in the computations. The recommended values of α in Table III are based on the results with an optimal basis up to the h symmetry (see the convergence Table VIII) and the estimated contribution from the i , j , and k symmetries. The combined contribution from i , j , and k symmetries are

$\approx 0.5\%$, 0.07% , and 0.02% , respectively, for Cn, Nh^+ , and Og. Although the contributions from the virtuals of symmetries higher than k are expected to be much smaller, we consider the highest contribution of 0.5% in the case of Cn as an upper bound from this source of uncertainty. The second source is the truncation of the dressed operator $\bar{\mathbf{D}}$ in the Eq. (8) to second order in $T^{(0)}$. In our previous work [47], we showed that the contribution from the remaining higher order terms is less than 0.1% . So, we consider this as the upper bound. The third source is the partial inclusion of the triple excitations in the PRCC theory. The partial triples contributions are $\approx 1.9\%$, 0.04% , and 0.5% of the PRCC values for Cn, Nh^+ , and Og, respectively. Since the perturbative triples subsumes the dominant contribution from triple excitations, we consider the highest contribution of 1.9% in the case Cn as an upper bound and the last source of theoretical uncertainty is associated with the frequency-dependent Breit interaction which is not included in the present paper. To estimate an upper bound of this source, we use the results in our previous work [33], where, using GRASP2K, we estimated an upper bound of

0.13% for Ra. Combining this with the Breit contributions, we determine $\approx 0.62\%$, 0.45% , and 0.18% as the contributions to Cn, Nh^+ and Og, respectively. Among these, we select the highest contribution of 0.62% from the case of Cn and take this as an upper bound. There could be other sources of theoretical uncertainties, such as the higher order coupled perturbation of vacuum polarization and self-energy terms, quadruply and higher excited cluster operators, etc. These, however, have much smaller contributions and their combined uncertainty could be below 0.1% . Finally, combining the upper bounds of all four sources of uncertainties, we estimate a theoretical uncertainty of 3.2% in the recommended values of α .

VI. CONCLUSION

We have employed a fully RCC theory to compute the ground state electric dipole polarizability and electron correlation energy of SHEs Cn, Nh^+ and Og. In addition, to understand the trend of electron correlation as function of Z , we have calculated the correlation energies of three lighter homologs for each SHEs. To improve the accuracy of our results, contributions from the Breit interaction, QED corrections and partial triple excitations are also included. Moreover, in all calculations, very large bases up to l -symmetry are used to check the convergence of the results.

Our recommended values of α for SHEs lie between the previous results, closer to the values from CCSD(T) [18,20] and RPA [17] calculations. From our calculations we find that the dominant contribution to α comes from the valence electrons, viz, $7s_{1/2}$ for both Cn and Nh^+ , and $7p_{3/2}$ for Og. While $7s_{1/2}$ contributes more than 50% of the total value for Cn and Nh^+ , the contribution from $7p_{3/2}$ orbital to Og is more than 95% . This could be attributed to the larger radial extent of these orbitals.

From the analysis of electron correlation effects, the core polarization effects decrease as a function of Z for the lighter homologs. For the SHEs, however, we observe an increased contribution. The corrections from the Breit interaction, except for Cn and Og, decrease as a function of Z . On the contrary, the Uehling potential and the self-energy corrections have increasing contributions from lighter homologs to SHEs. The largest contributions from the Uehling potential are $\approx 0.2\%$, 0.3% and 0.3% of the PRCC value for Cn, Nh^+ and Og, respectively. And, the same from the self-energy corrections are $\approx 0.4\%$, 0.2% and 0.1% , respectively. The combined Breit + QED corrections to α are observed to be $\approx 0.5\%$, 0.4% and 0.6% for Cn, Nh^+ and Og, respectively. Considering the importance of accurate properties of the SHEs, these are significant contributions, and can not be neglected.

ACKNOWLEDGMENTS

We would like to thank Chandan Kumar Vishwakarma for useful discussions. One of the authors, B.K.M., acknowledges funding support from the SERB (Grant No. ECR/2016/001454). The results presented in the paper are based on the computations using the High Performance Computing cluster, Padum, at the Indian Institute of Technology Delhi, New Delhi.

APPENDIX A: CONVERGENCE TABLE FOR α

In Table VIII, we provide the convergence trend of α as function of basis size. As is evident from the table, the value of α converges to 10^{-3} a.u. for all three SHEs.

APPENDIX B: SINGLE-ELECTRON ENERGIES

The single-electron energies of GTOs for SHEs Cn, Nh^+ , and Og are listed in the Tables IX–XI, respectively, and compared with the numerical data from GRASP2K [48] and the energies from the B-spline [54] basis. In Table XII, we list the contributions from the Breit interaction, Uehling potential, and the self-energy corrections to the single-electron energies.

TABLE XI. Orbital energies for core orbitals (in Hartree) from GTO compared with the GRASP2K and B-spline energies for Og. Here [x] represents multiplication by 10^x .

Orbital	GRASP2K	B spline	GTO
$1s_{1/2}$	8185.36230	8185.93230	8185.36258
$2s_{1/2}$	1718.80780	1718.93698	1718.80803
$3s_{1/2}$	471.19401	471.22553	471.19411
$4s_{1/2}$	140.97641	140.98548	140.97632
$5s_{1/2}$	39.88519	39.88767	39.88495
$6s_{1/2}$	8.98686	8.98760	8.98678
$7s_{1/2}$	1.29699	1.29711	1.29696
$2p_{1/2}$	1681.71710	1681.74523	1681.71618
$3p_{1/2}$	451.72699	451.73439	451.72665
$4p_{1/2}$	131.02105	131.02303	131.02069
$5p_{1/2}$	35.18375	35.18404	35.18340
$6p_{1/2}$	7.07694	7.07713	7.07689
$7p_{1/2}$	0.73956	0.73948	0.73944
$2p_{3/2}$	113.85447	113.854073	1138.54500
$3p_{3/2}$	318.33517	318.33345	318.33518
$4p_{3/2}$	92.02425	92.02349	92.02406
$5p_{3/2}$	23.66280	23.66234	23.66242
$6p_{3/2}$	4.21643	4.21630	4.21633
$7p_{3/2}$	0.30564	0.30564	0.30565
$3d_{3/2}$	286.65027	286.64895	286.65036
$4d_{3/2}$	76.26542	76.26467	76.26535
$5d_{3/2}$	16.66319	16.66277	16.66297
$6d_{3/2}$	1.76398	1.76387	1.76394
$3d_{5/2}$	265.67617	265.67496	265.67625
$4d_{5/2}$	70.35026	70.34956	70.35019
$5d_{5/2}$	15.07066	15.07028	15.07044
$6d_{5/2}$	1.49296	1.49285	1.49291
$4f_{5/2}$	49.79167	49.79139	49.79205
$5f_{5/2}$	6.51102	6.51097	6.51114
$4f_{7/2}$	48.04247	48.04220	48.04286
$5f_{7/2}$	6.14074	6.14070	6.14086

TABLE XII. The orbital energies for core orbitals from vacuum polarization and self-energy correction for Cn, Nh⁺, and Og.

Orbital	Cn				Nh ⁺		Og			
	$\Delta\epsilon_{Ue}$		$\Delta\epsilon_{SE}$		$\Delta\epsilon_{Ue}$	$\Delta\epsilon_{SE}$	$\Delta\epsilon_{Ue}$		$\Delta\epsilon_{SE}$	
	Ours	Ref. [55]	Ours	Ref. [55]	Ours	Ours	Ours	Ref. [55]	Ours	Ref. [55]
1s _{1/2}	-11.1193	-11.4416	30.6243	30.5752	-11.8402	31.9902	-16.2622	-16.7082	39.9045	39.7825
2s _{1/2}	-2.1505	-2.2283	5.9196	5.7672	-2.3160	6.2339	-3.3693	-3.4810	8.1051	7.7743
3s _{1/2}	-0.5193	-0.5410	1.4424	1.5061	-0.5597	1.5198	-0.8134	-0.8487	1.9781	2.1609
4s _{1/2}	-0.1494	-0.1560	0.4165	0.4375	-0.1614	0.4400	-0.2377	-0.2482	0.5795	0.6369
5s _{1/2}	-0.0436		0.1214		-0.0474	0.1291	-0.0718		0.1783	
6s _{1/2}	-0.0108		0.0297		-0.0119	0.0322	-0.0197		0.0500	
7s _{1/2}	-0.0015		0.0037		-0.0019	0.0047	-0.0040		0.0098	
2p _{1/2}	-0.5505	-0.6632	1.6011	1.6611	-0.6457	1.7455	-1.0858	-1.2661	2.7124	2.7853
3p _{1/2}	-0.1486	-0.1801	0.4445	0.5091	-0.1662	0.4835	-0.2926	-0.3430	0.7399	0.8812
4p _{1/2}	-0.0422	-0.0523	0.1278	0.1551	-0.0473	0.1394	-0.0845	-0.1010	0.2156	0.2712
5p _{1/2}	-0.0115		0.0359		-0.0130	0.0395	-0.0242		0.0674	
6p _{1/2}	-0.0024		0.0080		-0.0028	0.0090	-0.0059		0.0177	
7p _{1/2}							-0.0010		0.0027	
2p _{3/2}	0.0554	-0.0122	0.6914	0.6997	0.0594	0.7207	0.0848	-0.0169	0.8799	0.9013
3p _{3/2}	0.0183	-0.0038	0.1896	0.2002	0.0197	0.1983	0.0287	-0.0054	0.2476	0.2644
4p _{3/2}	0.0068	-0.0011	0.0565	0.0613	0.0074	0.0594	0.0110	-0.0017	0.0774	0.0827
5p _{3/2}	0.0026		0.0157		0.0028	0.0167	0.0043		0.0224	
6p _{3/2}	0.0009		0.0029		0.0010	0.0032	0.0016		0.0046	
7p _{3/2}								0.0003	0.0005	0.0445
3d _{3/2}	0.0205	-0.0001	-0.0015	-0.0014	0.0221	-0.0012	0.0316	-0.0002	0.0012	0.0012
4d _{3/2}	0.0070	0	-0.0005	0.0009	0.0076	-0.0004	0.0112	-0.0001	0.0004	0.0023
5d _{3/2}	0.0024		-0.0001		0.0026	-0.0001	0.0040		0.0001	
6d _{3/2}	0.0007		0		0.0007	0	0.0011		0	
3d _{5/2}	0.0185	0	0.0253	0.0231	0.0199	0.0265	0.0282	0	0.0333	0.0304
4d _{5/2}	0.0064	0	0.0084	0.0064	0.0069	0.0089	0.0102	0	0.0115	0.0086
5d _{5/2}	0.0022		0.0024		0.0024	0.0023	0.0036		0.0031	
6d _{5/2}	0.0006		0.0002		0.0006	0.0003	0.0010		0.0005	
4f _{5/2}	0.0055				0.0059		0.0088			
5f _{5/2}	0.0015				0.0017		0.0027			
4f _{7/2}	0.0053				0.0057		0.0084			
5f _{7/2}	0.0015				0.0016		0.0026			

- [1] A. Türler and V. Pershina, Advances in the production and chemistry of the heaviest elements, *Chem. Rev.* **113**, 1237 (2013).
- [2] M. Schädel, Chemistry of the superheavy elements, *Philos. Trans. R. Soc. A* **373**, 20140191 (2015).
- [3] V. Pershina, Electronic structure and properties of superheavy elements, *Nucl. Phys. A* **944**, 578 (2015), special issue on superheavy elements.
- [4] P. Schwerdtfeger, L. F. Pašteka, A. Punnett, and P. O. Bowman, Relativistic and quantum electrodynamic effects in superheavy elements, *Nucl. Phys. A* **944**, 551 (2015), special issue on superheavy elements.
- [5] E. Eliav, S. Fritzsche, and U. Kaldor, Electronic structure theory of the superheavy elements, *Nucl. Phys. A* **944**, 518 (2015), Special Issue on Superheavy Elements.
- [6] S. A. Giuliani, Z. Matheson, W. Nazarewicz, E. Olsen, P.-G. Reinhard, J. Sadhukhan, B. Schuetrumpf, N. Schunck, and P. Schwerdtfeger, Colloquium: Superheavy elements: Oganesson and beyond, *Rev. Mod. Phys.* **91**, 011001 (2019).
- [7] D. Shaughnessy and M. Schädel, *The Chemistry of the Superheavy Elements*, 2nd ed. (Springer, Heidelberg, 2014).
- [8] V. Pershina and D. C. Hoffman, *Transactinide Elements and Future Elements* (Springer, Dordrecht, 2008).
- [9] I. B. Khriplovich, *Parity Nonconservation in Atomic Phenomena* (Gordon and Breach Science Publishers, Philadelphia, 1991).
- [10] W. C. Griffith, M. D. Swallows, T. H. Loftus, M. V. Romalis, B. R. Heckel, and E. N. Fortson, Improved Limit on the Permanent Electric Dipole Moment of Hg¹⁹⁹, *Phys. Rev. Lett.* **102**, 101601 (2009).

- [11] Th. Udem, R. Holzwarth, and T. W. Hansch, Optical frequency metrology, *Nature (London)* **416**, 233 (2002).
- [12] M. Lewenstein, Ph. Balcou, M. Yu. Ivanov, A. L'Huillier, and P. B. Corkum, Theory of high-harmonic generation by low-frequency laser fields, *Phys. Rev. A* **49**, 2117 (1994).
- [13] M. H. Anderson, J. R. Ensher, M. R. Matthews, C. E. Wieman, and E. A. Cornell, Observation of Bose-Einstein condensation in a dilute atomic vapor, *Science* **269**, 198 (1995).
- [14] S. G. Karshenboim and E. Peik, *Astrophysics, Clocks and Fundamental Constants*, Lecture Notes in Physics (Springer, New York, 2010).
- [15] M. Seth, P. Schwerdtfeger, and M. Dolg, The chemistry of the superheavy elements. I. Pseudopotentials for 111 and 112 and relativistic coupled cluster calculations for (112)h+, (112)f2, and (112)f4, *J. Chem. Phys.* **106**, 3623 (1997).
- [16] C. S. Nash, Atomic and molecular properties of elements 112, 114, and 118, *J. Phys. Chem. A* **109**, 3493 (2005).
- [17] V. A. Dzuba, Ionization potentials and polarizabilities of superheavy elements from Db to Cn ($Z=105-112$), *Phys. Rev. A* **93**, 032519 (2016).
- [18] V. Pershina, A. Borschevsky, E. Eliav, and U. Kaldor, Prediction of the adsorption behavior of elements 112 and 114 on inert surfaces from *ab initio* Dirac-Coulomb atomic calculations, *J. Chem. Phys.* **128**, 024707 (2008).
- [19] V. Pershina, A. Borschevsky, E. Eliav, and U. Kaldor, Adsorption of inert gases including element 118 on noble metal and inert surfaces from *ab initio* Dirac-Coulomb atomic calculations, *J. Chem. Phys.* **129**, 144106 (2008).
- [20] P. Jerabek, B. Schuettrumpf, P. Schwerdtfeger, and W. Nazarewicz, Electron and Nucleon Localization Functions of Oganesson: Approaching the Thomas-Fermi Limit, *Phys. Rev. Lett.* **120**, 053001 (2018).
- [21] Yu. Ts. Oganessian, V. K. Utyonkov, Yu. V. Lobanov, F. Sh. Abdullin, A. N. Polyakov, R. N. Sagaidak, I. V. Shirokovsky, Yu. S. Tsyganov, A. A. Voinov, G. G. Gulbekian, S. L. Bogomolov, B. N. Gikal, A. N. Mezentsev, S. Iliev, V. G. Subbotin, A. M. Sukhov, K. Subotic, V. I. Zagrebaev, G. K. Vostokin, M. G. Itkis *et al.*, Synthesis of the isotopes of elements 118 and 116 in the ^{249}Cf and $^{245}\text{Cm} + ^{48}\text{Ca}$ fusion reactions, *Phys. Rev. C* **74**, 044602 (2006).
- [22] P. J. Karol, R. C. Barber, B. M. Sherrill, E. Vardaci, and T. Yamazaki, Discovery of the element with atomic number $Z = 118$ completing the 7th row of the periodic table (IUPAC technical report), *Pure Appl. Chem.* **88**, 155 (2016).
- [23] S. Hofmann, V. Ninov, F. P. Heßberger, P. Armbruster, H. Folger, G. Münzenberg, H. J. Schött, A. G. Popeko, A. V. Yeremin, S. Saro, R. Janik, and M. Leino, The new element 112, *Z. Phys. A* **354**, 229 (1996).
- [24] Yu. Ts. Oganessian, A. V. Yeremin, A. G. Popeko, S. L. Bogomolov, G. V. Buklanov, M. L. Chelnokov, V. I. Chepigin, B. N. Gikal, V. A. Gorshkov, G. G. Gulbekian, M. G. Itkis, A. P. Kabachenko, A. Yu. Lavrentev, O. N. Malyshev, J. Rohac, R. N. Sagaidak, S. Hofmann, S. Saro, G. Giardina, and K. Morita, Synthesis of nuclei of the superheavy element 114 in reactions induced by ^{48}Ca , *Nature (London)* **400**, 242 (1999).
- [25] Yu. Ts. Oganessian, A. V. Yeremin, A. G. Popeko, O. N. Malyshev, A. V. Belozerov, G. V. Buklanov, M. L. Chelnokov, V. I. Chepigin, V. A. Gorshkov, S. Hofmann, M. G. Itkis, A. P. Kabachenko, B. Kindler, G. Münzenberg, R. N. Sagaidak, Š Šáro, H.-J. Schött, B. Štreicher, A. V. Shutov, A. I. Svirikhin *et al.*, Second experiment at Vassilissa separator on the synthesis of the element 112, *Eur. Phys. J. A* **19**, 3 (2004).
- [26] Yu. Ts. Oganessian, V. K. Utyonkov, Yu. V. Lobanov, F. Sh. Abdullin, A. N. Polyakov, I. V. Shirokovsky, Yu. S. Tsyganov, G. G. Gulbekian, S. L. Bogomolov, B. N. Gikal, A. N. Mezentsev, S. Iliev, V. G. Subbotin, A. M. Sukhov, A. A. Voinov, G. V. Buklanov, K. Subotic, V. I. Zagrebaev, M. G. Itkis, J. B. Patin *et al.*, Measurements of cross sections and decay properties of the isotopes of elements 112, 114, and 116 produced in the fusion reactions $^{233,238}\text{U}$, ^{242}Pu , and $^{248}\text{Cm} + ^{48}\text{Ca}$, *Phys. Rev. C* **70**, 064609 (2004).
- [27] R. Eichler, N. V. Aksenov, A. V. Belozerov, G. A. Bozhikov, V. I. Chepigin, S. N. Dmitriev, R. Dressler, H. W. Gäggeler, V. A. Gorshkov, F. Haenssler, M. G. Itkis, A. Laube, V. Ya. Lebedev, O. N. Malyshev, Yu. Ts. Oganessian, O. V. Petrushkin, D. Piguët, P. Rasmussen, S. V. Shishkin, A. V. Shutov *et al.*, Chemical characterization of element 112, *Nature (London)* **447**, 72 (2007).
- [28] K. Morita, K. Morimoto, D. Kaji, T. Akiyama, Sin-ichi Goto, H. Haba, E. Ideguchi, R. Kanungo, K. Katori, H. Koura, H. Kudo, T. Ohnishi, A. Ozawa, T. Suda, K. Sueki, H. Xu, T. Yamaguchi, A. Yoneda, A. Yoshida, and Y. Zhao, Experiment on the synthesis of element 113 in the reaction $^{209}\text{Bi}(^{70}\text{Zn}, n)^{278}113$, *J. Phys. Soc. Jpn.* **73**, 2593 (2004).
- [29] S. Chattopadhyay, B. K. Mani, and D. Angom, Triple excitations in perturbed relativistic coupled-cluster theory and electric dipole polarizability of group-IIB elements, *Phys. Rev. A* **91**, 052504 (2015).
- [30] R. Kumar, S. Chattopadhyay, B. K. Mani, and D. Angom, Electric dipole polarizability of group-13 ions using perturbed relativistic coupled-cluster theory: Importance of nonlinear terms, *Phys. Rev. A* **101**, 012503 (2020).
- [31] S. Chattopadhyay, B. K. Mani, and D. Angom, Perturbed coupled-cluster theory to calculate dipole polarizabilities of closed-shell systems: Application to Ar, Kr, Xe, and Rn, *Phys. Rev. A* **86**, 062508 (2012).
- [32] S. Chattopadhyay, B. K. Mani, and D. Angom, Electric dipole polarizabilities of doubly ionized alkaline-earth-metal ions from perturbed relativistic coupled-cluster theory, *Phys. Rev. A* **87**, 062504 (2013).
- [33] S. Chattopadhyay, B. K. Mani, and D. Angom, Electric dipole polarizability of alkaline-earth-metal atoms from perturbed relativistic coupled-cluster theory with triples, *Phys. Rev. A* **89**, 022506 (2014).
- [34] M. S. Safronova, W. R. Johnson, and A. Derevianko, Relativistic many-body calculations of energy levels, hyperfine constants, electric-dipole matrix elements, and static polarizabilities for alkali-metal atoms, *Phys. Rev. A* **60**, 4476 (1999).
- [35] A. Derevianko, W. R. Johnson, M. S. Safronova, and J. F. Babb, High-Precision Calculations of Dispersion Coefficients, Static Dipole Polarizabilities, and Atom-Wall Interaction Constants for Alkali-Metal Atoms, *Phys. Rev. Lett.* **82**, 3589 (1999).
- [36] J. Sucher, Foundations of the relativistic theory of many-electron atoms, *Phys. Rev. A* **22**, 348 (1980).
- [37] J. Mitroy, M. S. Safronova, and C. W. Clark, Theory and applications of atomic and ionic polarizabilities, *J. Phys. B: At., Mol. Opt. Phys.* **43**, 202001 (2010).
- [38] <http://ctcp.massey.ac.nz/dipole-polarizabilities>.
- [39] A. K. Mohanty, F. A. Parpia, and E. Clementi, Kinetically balanced geometric Gaussian basis set calculations for relativistic

- many-electron atoms, in *Modern Techniques in Computational Chemistry: MOTECC-91*, edited by E. Clementi (Scientific and Engineering Computations, New York, 1991).
- [40] R. E. Stanton and S. Havriliak, Kinetic balance: A partial solution to the problem of variational safety in Dirac calculations, *J. Chem. Phys.* **81**, 1910 (1984).
- [41] I. P. Grant, *Relativistic Quantum Theory of Atoms and Molecules: Theory and Computation* (Springer, New York, 2010).
- [42] I. Grant, Relativistic atomic structure, in *Springer Handbook of Atomic, Molecular, and Optical Physics*, edited by G. Drake (Springer, New York, 2006), pp. 325–357.
- [43] I. P. Grant and B. J. McKenzie, The transverse electron-electron interaction in atomic structure calculations, *J. Phys. B* **13**, 2671 (1980).
- [44] S. Chattopadhyay, B. K. Mani, and D. Angom, Electric dipole polarizability from perturbed relativistic coupled-cluster theory: Application to neon, *Phys. Rev. A* **86**, 022522 (2012).
- [45] S. Chattopadhyay, B. K. Mani, and D. Angom, Electric dipole polarizabilities of alkali-metal ions from perturbed relativistic coupled-cluster theory, *Phys. Rev. A* **87**, 042520 (2013).
- [46] G. D. Purvis and R. J. Bartlett, A full coupled-cluster singles and doubles model: The inclusion of disconnected triples, *J. Chem. Phys.* **76**, 1910 (1982).
- [47] B. K. Mani and D. Angom, Atomic properties calculated by relativistic coupled-cluster theory without truncation: Hyperfine constants of Mg^+ , Ca^+ , Sr^+ , and Ba^+ , *Phys. Rev. A* **81**, 042514 (2010).
- [48] P. Jönsson, G. Gaigalas, J. Bieroń, C. Froese Fischer, and I. P. Grant, New version: Grasp2k relativistic atomic structure package, *Comput. Phys. Commun.* **184**, 2197 (2013).
- [49] E. A. Uehling, Polarization effects in the positron theory, *Phys. Rev.* **48**, 55 (1935).
- [50] L. Wayne Fullerton and G. A. Rinker, Accurate and efficient methods for the evaluation of vacuum-polarization potentials of order $z\alpha$ and $z\alpha^2$, *Phys. Rev. A* **13**, 1283 (1976).
- [51] S. Klarsfeld, Analytical expressions for the evaluation of vacuum-polarization potentials in muonic atoms, *Phys. Lett. B* **66**, 86 (1977).
- [52] V. M. Shabaev, I. I. Tupitsyn, and V. A. Yerokhin, Model operator approach to the lamb shift calculations in relativistic many-electron atoms, *Phys. Rev. A* **88**, 012513 (2013).
- [53] V. M. Shabaev, I. I. Tupitsyn, and V. A. Yerokhin, Qedmod: Fortran program for calculating the model lamb-shift operator, *Comput. Phys. Commun.* **189**, 175 (2015).
- [54] O. Zatsarinny and C. Froese Fischer, DBSR-HF: A B-spline Dirac-Hartree-Fock program, *Comput. Phys. Commun.* **202**, 287 (2016).
- [55] K. Koziol and G. A. Aucar, Qed effects on individual atomic orbital energies, *J. Chem. Phys.* **148**, 134101 (2018).
- [56] B. K. Mani, S. Chattopadhyay, and D. Angom, Rccpac: A parallel relativistic coupled-cluster program for closed-shell and one-valence atoms and ions in fortran, *Comput. Phys. Commun.* **213**, 136 (2017).
- [57] J. R. Flores and P. Redondo, Computation of second-order correlation energies using a finite element method for atoms with d electrons, *J. Phys. B: At., Mol. Opt. Phys.* **26**, 2251 (1993).
- [58] J. R. Flores and P. Redondo, High-precision atomic computations from finite element techniques: Second-order correlation energies for Be, Ca, Sr, Cd, Ba, Yb, and Hg, *J. Comput. Chem.* **15**, 782 (1994).
- [59] J. R. Flores, High precision atomic computations from finite element techniques: Second-order correlation energies of rare gas atoms, *J. Chem. Phys.* **98**, 5642 (1993).
- [60] Y. Ishikawa and K. Koc, Relativistic many-body perturbation theory based on the no-pair Dirac-Coulomb-Breit Hamiltonian: Relativistic correlation energies for the noble-gas sequence through Rn ($Z=86$), the group-IIb atoms through Hg, and the ions of Ne isoelectronic sequence, *Phys. Rev. A* **50**, 4733 (1994).
- [61] B. K. Mani, K. V. P. Latha, and D. Angom, Relativistic coupled-cluster calculations of ^{20}Ne , ^{40}Ar , ^{84}Kr , and ^{129}Xe : Correlation energies and dipole polarizabilities, *Phys. Rev. A* **80**, 062505 (2009).
- [62] S. P. McCarthy and A. J. Thakkar, Accurate all-electron correlation energies for the closed-shell atoms from Ar to Rn and their relationship to the corresponding MP2 correlation energies, *J. Chem. Phys.* **134**, 044102 (2011).
- [63] A. Ye and G. Wang, Dipole polarizabilities of $ns^2\ ^1S_0$ and $nsnp\ ^3P_0$ states and relevant magic wavelengths of group-IIb atoms, *Phys. Rev. A* **78**, 014502 (2008).
- [64] R. Roos, Björn O. and Lindh, P. Malmqvist, V. Veryazov, and P.-O. Widmark, New relativistic ANO basis sets for transition metal atoms, *J. Phys. Chem. A* **109**, 6575 (2005).
- [65] P. Schwerdtfeger, J. Li, and P. Pykkö, The polarisability of Hg and the ground-state interaction potential of Hg_2 , *Theor. Chim. Acta* **87**, 313 (1994).
- [66] V. Kellö and A. J. Sadlej, Polarized basis sets for high-level-correlated calculations of molecular electric properties, *Theor. Chim. Acta* **91**, 353 (1995).
- [67] H. Hachisu, K. Miyagishi, S. G. Porsev, A. Derevianko, V. D. Ovsiannikov, V. G. Pal'chikov, M. Takamoto, and H. Katori, Trapping of Neutral Mercury Atoms and Prospects for Optical Lattice Clocks, *Phys. Rev. Lett.* **100**, 053001 (2008).
- [68] Y. Singh and B. K. Sahoo, Rigorous limits on the hadronic and semileptonic CP -violating coupling constants from the electric dipole moment of ^{199}Hg , *Phys. Rev. A* **91**, 030501(R) (2015).
- [69] K. T. Tang and J. P. Toennies, The dynamical polarisability and van der Waals dimer potential of mercury, *Mol. Phys.* **106**, 1645 (2008).
- [70] D. Goebel and U. Hohm, Dipole Polarizability, Cauchy moments, and related properties of Hg, *J. Phys. Chem.* **100**, 7710 (1996).
- [71] A. M. Dyugaev and E. V. Lebedeva, New qualitative results of the atomic theory, *JETP Lett.* **104**, 639 (2016).
- [72] V. Kellö and A. J. Sadlej, Standardized basis sets for high-level-correlated relativistic calculations of atomic and molecular electric properties in the spin-averaged Douglas-Kroll (no-pair) approximation I. Groups Ib and IIb, *Theor. Chim. Acta* **94**, 93 (1996).
- [73] B. K. Sahoo and B. P. Das, Relativistic Normal Coupled-Cluster Theory for Accurate Determination of Electric Dipole Moments of Atoms: First Application to the ^{199}Hg Atom, *Phys. Rev. Lett.* **120**, 203001 (2018).
- [74] B. K. Sahoo and B. P. Das, The role of relativistic many-body theory in probing new physics beyond the standard model via the electric dipole moments of diamagnetic atoms, *J. Phys.: Conf. Ser.* **1041**, 012014 (2018).

- [75] Z. Zuhrianda, M. S. Safronova, and M. G. Kozlov, Anomalously small blackbody radiation shift in the Tl^+ frequency standard, *Phys. Rev. A* **85**, 022513 (2012).
- [76] N. Reshetnikov, L. J. Curtis, M. S. Brown, and R. E. Irving, Determination of polarizabilities and lifetimes for the Mg, Zn, Cd and Hg isoelectronic sequences, *Phys. Scr.* **77**, 015301 (2008).
- [77] T. Nakajima and K. Hirao, Relativistic effects for polarizabilities and hyperpolarizabilities of rare gas atoms, *Chem. Lett.* **30**, 766 (2001).
- [78] P. Soldán, E. P. F. Lee, and T. G. Wright, Static dipole polarizabilities (α) and static second hyperpolarizabilities (γ) of the rare gas atoms (He-Rn), *Phys. Chem. Chem. Phys.* **3**, 4661 (2001).
- [79] B. O. Roos, R. Lindh, P. Malmqvist, V. Veryazov, and P.-O. Widmark, Main group atoms and dimers studied with a new relativistic ANO basis set, *J. Phys. Chem. A* **108**, 2851 (2004).
- [80] N. P. Labello, A. M. Ferreira, and H. A. Kurtz, An augmented effective core potential basis set for the calculation of molecular polarizabilities, *J. Comput. Chem.* **26**, 1464 (2005).
- [81] D. Sulzer, P. Norman, and T. Saue, Atomic C_6 dispersion coefficients: A four-component relativistic Kohn–Sham study, *Mol. Phys.* **110**, 2535 (2012).
- [82] D. A. Pantazis and F. Neese, All-electron scalar relativistic basis sets for the $6p$ elements, *Theor. Chem. Acc.* **131**, 1292 (2012).
- [83] N. Runeberg and P. Pyykko, Relativistic pseudopotential calculations on Xe_2 , $RnXe$, and Rn_2 : The van der Waals properties of radon, *Int. J. Quantum Chem.* **66**, 131 (1998).